

Ground-State Properties of Nonspherical Nuclei*

KURT GOTTFRIED†

*Laboratory for Nuclear Science, Massachusetts Institute of Technology, Cambridge, Massachusetts,
and Department of Physics, Harvard University, Cambridge, Massachusetts*

(Received March 1, 1956)

A knowledge of the wave functions and energy levels for nucleonic motion in a nonspherical force field is a prerequisite to any detailed comparison between the empirical data and the model of Bohr and Mottelson. An extremely simple model for this internal problem is provided by the motion of independent particles in an ellipsoidal oscillator potential. By minimizing the total energy of such a system, we are led to conclude (1) that deformations which possess an axis of symmetry are always preferred by low-lying states, and (2) that this model cannot reproduce the observed preponderance of positive quadrupole moments. This last conclusion is unaltered by the surface tension or Coulomb repulsion.

The oscillator model is too simplified for the computation of spins or magnetic moments (μ). We have therefore determined wave functions and energy levels for independent-particle motion in a spheroidal square well, including spin-orbit coupling. Because of the approximations made in this calculation, we cannot use our levels to compute the equilibrium shape, but only to assign

the ground-state level and wave function. Thus the present scheme is intended to replace that of the shell model in the region of large deformations.

With the exception of W^{183} , we have been able to correctly assign the spin to all the odd- A nuclei for which $150 \lesssim A \lesssim 190$. The ease and consistency with which such an assignment can be made leads us to conclude that our scheme is essentially correct for those nuclei which possess large deformations, and whose odd particle lies in the 50-82 shell or the lower part of the 82-126 shell. In addition, we have computed μ in this region. Here the agreement is more limited, but there are a number of important successes: we reproduce the large difference in μ for the europium isotopes, the ratio of the magnetic moments of the two hafnium isotopes, both μ and the decoupling coefficient for Tm^{169} , and μ for $Yb^{171,173}$, Re , Eu^{161} , and Os^{189} . The properties of the ground state and first excited state of Ag^{109} are also found to be in good agreement with the theory.

I. INTRODUCTION

THE concept that nuclei can be nonspherical in shape had its origin in the failure of the shell model to account for the extremely large quadrupole moments found among the rare earths.¹ For "shell model" implies that only a few nucleons can contribute to the moment, while the data show that a considerable portion of the total nuclear charge must be participating in the formation of the quadrupole moment. Rainwater² proposed to resolve this difficulty with the assumption that, in these cases, the nuclear collective field with which the shell model operates is not spherical, but spheroidal in shape, as a consequence of which one expects the majority of the proton orbits to contribute to the quadrupole moment (henceforth designated by Q).

Although Rainwater's qualitative considerations were quite promising, the very assumption of nonsphericity leads to complications whose full significance was first realized³ and analyzed⁴ by Bohr. Among these new complexities the most important and understandable one is that the angular momentum J of particles moving in a nonspherical field is not a constant of

motion, and so the system must possess some other angular momentum N which is coupled to J , and results in a conserved total angular momentum I . The angular momentum N is associated with collective rotation of nuclear matter. Another complication is due to the fact that the shape of a quantum mechanical system cannot be defined with arbitrary accuracy, and so there must be zero-point oscillations of this shape about some equilibrium configuration. These oscillations are, by definition, also collective in nature. Both these collective motions are coupled to that of the individual particles, and also to each other.

Bohr and Mottelson^{4,5} have analyzed the motion of such a coupled system in several limiting situations. The most interesting is the one in which the motion separates approximately (Born-Oppenheimer approximation) into three parts: (1) motion of nucleons in a static, nonspherical potential, (2) collective rotation, and (3) oscillation about the static equilibrium deformation.⁶ As in molecules, there are three distinct types of excitations: rotational, nucleonic and vibrational, in ascending magnitude of energy. The wave function can then be written as the product of three functions, each factor representing one mode of the motion, and the first few steps in the spectrum follow the well-known rules applicable to a rotating top.⁷ The empirical data⁸ support this conclusion—in fact the experimental

* This work was partially supported by the Office of Naval Research and the U. S. Atomic Energy Commission.

† Junior Fellow, Society of Fellows. Present address: Jefferson Physical Laboratory, Harvard University, Cambridge, Massachusetts.

¹ We now know that nuclei much heavier than Pb^{208} also have giant quadrupole moments. Therefore this discussion, unless otherwise stated, pertains to nuclei with mass number $A \gtrsim 225$, as well as $150 \lesssim A \lesssim 190$, i.e., to heavy nuclei well removed from the magic numbers.

² J. Rainwater, *Phys. Rev.* **79**, 432 (1950).

³ A. Bohr, *Phys. Rev.* **81**, 134 (1951).

⁴ A. Bohr, *Kgl. Danske Videnskab. Selskab, Mat.-fys. Medd.* **26**, No. 14 (1952).

⁵ A. Bohr and B. R. Mottelson, *Kgl. Danske Videnskab. Selskab, Mat.-fys. Medd.* **27**, No. 16 (1953). Also see A. Reifman, *Z. Naturforsch.* **8a**, 505 (1953); D. L. Hill and J. A. Wheeler, *Phys. Rev.* **89**, 1102 (1953); K. W. Ford, *Phys. Rev.* **90**, 29 (1953).

⁶ Bohr calls this the "strong-coupling" approximation.

⁷ C. Van Winter, *Physica* **20**, 274 (1954).

⁸ A. Bohr and B. R. Mottelson, *Beta- and Gamma-Ray Spectroscopy*, edited by K. Siegbahn (North-Holland Publishing Company, Amsterdam, 1955), pp. 483-493.

spectra faithfully obey the interval rule characteristic of a symmetric rotor. This property of the level spacing, and the values of the branching ratios⁸ of γ transitions between and β decays to components of a rotational band, show that these low-lying states can be represented by the wave function

$$\Psi_{kK\Omega M}^{(I)} = (I + \frac{1}{2})^{\frac{1}{2}} \mathcal{G} [\mathcal{D}_{MK}^{(I)*} \chi_{k, \Omega} + (-1)^{I-\frac{1}{2}} \mathcal{D}_{M-K}^{(I)*} \chi_{k, -\Omega}]. \quad (1)$$

Here \mathcal{G} is the wave function of the zero-point vibrations; $\mathcal{D}_{MK}^{(I)}$ is an element of the $(2I+1)$ -dimensional representation of the rotation group, and $\chi_{k, \Omega}$ is the wave function of the nucleonic motion in the spheroidal force-field. Because of the axial symmetry of the deformation, the particles' angular momentum along the body-fixed symmetry axis is a constant of the motion, which we designate by Ω . The other quantum numbers I, K, M stand for the total angular momentum, its component along the symmetry axis and its component along a space-fixed z' -axis respectively, while k serves to distinguish the various χ 's which have the same value of $|\Omega|$.

The lowest states are characterized by $K=\Omega$, and their energy differences are given by

$$\Delta E_I = \frac{\hbar^2}{2\mathcal{J}} [I(I+1) - I_0(I_0+1)], \quad (2)$$

where I_0 is the spin of the ground state and \mathcal{J} is the effective moment of inertia. For even-even nuclei, $|\Omega|=I_0=0$ and $I=2, 4$, etc.; for odd- A nuclei, $|\Omega|=I_0$ and $I=I_0+1, I_0+2$, etc., unless $|\Omega|=\frac{1}{2}$. In the latter case the Coriolis force must be taken into account, and this leads to the expression⁹

$$\frac{\hbar^2}{2\mathcal{J}} a_k [(-1)^{I+\frac{1}{2}} (I + \frac{1}{2}) - (-1)^{I_0+\frac{1}{2}} (I_0 + \frac{1}{2})] \delta_{|\Omega|, \frac{1}{2}}, \quad (3)$$

which is to be added to ΔE_I . Here

$$a_k = \langle \chi_{k, \Omega=\frac{1}{2}} | J_x + iJ_y | \chi_{k, \Omega=-\frac{1}{2}} \rangle, \quad (4)$$

where J_x, J_y are the components of the particles' angular momentum along the body-fixed x - and y -axis respectively. Furthermore, I_0 depends on the value of a_k ¹⁰; it is not one-half in general.

It is to be noted that beyond the general structure of the state (1), the spectral intervals and branching ratios determine only \mathcal{J} , I_0 and sometimes a_k . Of these, \mathcal{J} may be termed an extensive observable, since it depends on the over-all nature of the collective rotation,¹¹ and not so sensitively on the detailed properties of χ . On the other hand, a_k provides an effective probe into the structure of χ , while the assignment of I_0

depends on the properties of the internal Hamiltonian which has the χ 's as eigenstates.

There is a considerable mass of empirical material which sheds further light on the nature of both the collective and particle motion. This material is conveniently separated into two broad but somewhat overlapping classes, the first pertaining essentially to the collective, the second more to the particle aspects of the motion. Experiments belonging to the first class demonstrate that for the nuclei under consideration not only Q , but also the matrix elements for induced and spontaneous $E2$ transitions are far larger than the shell-model estimates, and that \mathcal{J} is roughly proportional to Q^2 , the proportionality factor indicating that the rotation is neither rigid nor irrotational.¹² The details of the structure of χ are revealed only by data of the second class, which includes the magnetic moments, the electromagnetic transition probabilities other than the $E2$ -type, β -decay ft values, and the energy differences between rotational bands.¹³

It is apparent that a knowledge of the intrinsic (or nucleonic) wave function χ is a prerequisite to a comprehensive comparison between the model and data. In the following we shall construct a set of χ 's from a model of the intrinsic motion which embodies, among others, the great simplification that the internucleon forces may be ignored, i.e., the particles are assumed to move independently of each other under the influence of the collective field. This assumption is certainly a drastic one, but the successes of the shell¹³ and optical¹⁴ models indicate that it is at least a reasonable starting point. In addition, we will always assume that the equipotential surfaces of the collective field are confocal ellipsoids whose volume, for the sake of nuclear incompressibility, is independent of the eccentricities. These geometrical assumptions are probably well justified for low-lying states, and simplify the computations considerably. Finally, we shall also assume that the conditions of constraint implicit in the introduction of collective variables¹⁵ may be ignored.

Even though our first and most essential idealization—that of independent motion—is not entirely justifiable,¹¹ our work is not in vain since a more realistic determination of the χ 's might have to use a crude set of functions such as we shall construct as the basis of a perturbation calculation.

In the following section we briefly consider an

¹² The interaction between the collective and nucleonic degrees of freedom is, of course, reflected in the experimental results and, as stated above, renders the attempted separation of the data somewhat ambiguous; thus, for example, the total g -factor has contributions from both the collective and nucleonic rotations, as do the ($E2:M1$) admixtures of radiative transitions between rotational states. Nevertheless, this classification serves the didactic purpose of focusing our attention on the most essential physical attribute of each phenomenon under investigation.

¹³ See, e.g., P. F. A. Klinkenberg, *Revs. Modern Phys.* **24**, 63 (1952).

¹⁴ Feshbach, Porter, and Weisskopf, *Phys. Rev.* **96**, 448 (1954).

¹⁵ F. Coester, *Phys. Rev.* **99**, 170 (1955); Lipkin, deShalit, and Talmi, *Nuovo cimento* **2**, 773 (1955); F. Villars (to be published).

⁹ J. P. Davidson and E. Feenberg, *Phys. Rev.* **89**, 856 (1953).

¹⁰ See, e.g., S. G. Nilsson, *Kgl. Danske Videnskab. Selskab, Mat.-fys. Medd.* **29**, No. 16, 68 (1955).

¹¹ A. Bohr and B. R. Mottelson, *Kgl. Danske Videnskab. Selskab, Mat.-fys. Medd.* **30**, No. 1 (1955).

extremely simple model whose properties can be evaluated analytically, and which serves as a very useful orientation for the problem at hand. The wave functions and energy levels belonging to a more realistic collective potential are discussed in Sec. III, and selected application to nuclear ground-state properties will be found in Sec. IV.

II. HARMONIC OSCILLATOR MODEL

A systematic study of Q and \mathcal{J} reveals a striking correlation between the nuclear shell structure and equilibrium deformation^{8,16}: the distortion becomes very small near the magic numbers and is largest in the middle of major shells. From this we conclude that the shell structure of the nuclear level scheme is, for our purpose, a most essential feature which we must incorporate into the model. Since the harmonic oscillator (without spin-orbit coupling) is the simplest collective potential which exhibits a shell structure, we shall employ it as a first orientation.¹⁷⁻¹⁹ The exclusion of the spin-orbit force implies that this model cannot be used to assign spins and magnetic moments. Nevertheless, we may still expect to gain some insight into the question of nuclear deformability, and so we confine ourselves to this problem for the moment.

The most general potential of the oscillator type which fulfills the requirement of incompressibility is

$$V(\mathbf{r}) = \frac{1}{2}m\omega^2[(x^2\gamma^2 + y^2\gamma^{-2})\lambda + z^2\lambda^{-2}], \quad (0 \leq \lambda \leq \infty, 0 \leq \gamma \leq \infty), \quad (5)$$

where ω is the oscillator's frequency, m the nucleon mass, and \mathbf{r} the position vector in the rotating coordinate system. The dimensionless deformation parameters γ, λ are related to the eccentricities in the x - y and y - z planes through

$$\mathcal{E}_{xy}^2 = \gamma^4 - 1; \quad \mathcal{E}_{yz}^2 = \lambda^{-3}(\lambda^3 - \gamma^2). \quad (6)$$

The equipotential surfaces are symmetric about the x , y , or z axis when $\gamma = \lambda^{\frac{1}{2}}$, $\lambda^{-\frac{1}{2}}$, or 1, respectively. In the latter case $\lambda > 1$ corresponds to a prolate, $\lambda < 1$ to an oblate spheroid.

Our aim is to find the nuclear equilibrium deformation when the potential (5) is occupied by Z protons and $(A-Z)$ neutrons. This configuration is clearly given by those values of γ and λ which minimize the total energy. This energy is not simply the energy of the particles in the collective field $E_P(\gamma, \lambda)$, but also has contributions from the Coulomb repulsion and more subtle sources such as the surface effect.²⁰ We will designate these last two contributions to the energy by $E_C(\gamma, \lambda)$ and $E_S(\gamma, \lambda)$ respectively.

The observation that $E_P(\gamma, \lambda)$ has an average curvature roughly equal to the one expected from the semiempirical mass formula has led some authors¹⁸ to conclude that E_P already includes the surface effect. This argument is not convincing because (1) the values of λ for which E_P attains this average curvature are for larger than those realized in nature, and (2) for such large values of λ the conventional power series expressions for E_S and E_C fail. In any case, the well-known argument that the suppression of nucleon-nucleon bonding at the surface leads to a "surface-tension" is still pertinent today, and does not hinge on the demise of the liquid drop model. On the other hand, a literal interpretation of the mass formula in terms of liquid drop concepts is dangerous. To summarize, we would say (a) that one should expect some surface energy E_S above and beyond E_P , and (b) that one should not expect its strength to be given by the $A^{\frac{1}{3}}$ term in the semiempirical mass formula.

As for the particle energy, it is given simply by

$$E_P(\gamma, \lambda) = \sum_{i=1}^A \left[\left\langle -\frac{\hbar^2}{2m} \nabla_i^2 \right\rangle_i + \frac{1}{2} \langle V(\mathbf{r}_i) \rangle_i \right], \quad (7)$$

where the index i labels the i th nucleon. The factor of one-half preceding the expectation value of $V(\mathbf{r})$ expresses the assumption that the basic interactions which coalesce to form the collective field are two-body forces.²¹ The expectation values in (7) are elementary; one finds that

$$E_P(\gamma, \lambda) = \frac{3}{4}\hbar\omega[(\mathcal{Q}_x\gamma + \mathcal{Q}_y\gamma^{-1})\lambda^{\frac{1}{2}} + \frac{1}{2}\mathcal{B}\lambda^{-1}], \quad (8)$$

where

$$\mathcal{Q}_x = \sum_{i=1}^A (n_x^i + \frac{1}{2}), \quad \mathcal{Q}_y = \sum_{i=1}^A (n_y^i + \frac{1}{2}), \quad (9)$$

$$\mathcal{B} = 2 \sum_{i=1}^A (n_z^i + \frac{1}{2}),$$

and the n 's are the usual oscillator quantum numbers.

For the sake of clarity, we shall now approach our problem in a series of steps of ascending complexity. That is, we begin by ignoring the Coulomb and surface effects, and allow only one species of nucleons to fill the potential well (5). This will be followed by a discussion where both neutrons and protons are considered. Finally, we will study the effect of the Coulomb and surface energies on Q .

When $E_S = E_C = 0$, the total energy is simply E_P [see Eq. (8)]. The values of (γ_0, λ_0) which minimize $E_P(\gamma, \lambda)$ as consecutive orbitals in the $N = n_x + n_y + n_z = 4$ shell are filled with pairs of particles is given in Table I.

¹⁶ Townes, Foley, and Low, Phys. Rev. **76**, 1415 (1949).

¹⁷ D. Pfirsich, Z. Physik **132**, 409 (1952).

¹⁸ S. Gallone and C. Salvetti, Nuovo cimento **10**, 145 (1953).

¹⁹ M. Gursky, Phys. Rev. **98**, 1205(A) (1955).

²⁰ Because of the adiabatic assumption underlying the "strong-coupling" approximation, one may ignore the rotational energy when determining the equilibrium energy.

²¹ See, e.g., E. U. Condon and G. H. Shortley, *Theory of Atomic Spectra* (Cambridge University Press, Cambridge, 1935), Sec. 8.¹⁴ If three-body forces are of importance, one would have to know the relative strengths of the two- and three-body potentials before one could compute E_P . The author is indebted to Dr. C. Schwartz for bringing this point to his attention.

TABLE I. Deformation parameters as a function of A .

A	α_x	α_y	β	λ_0	γ_0	\mathcal{E}_{xy}^2	$\delta Q(\%)^a$
40+0	50+0	50+0	50+0	1.000	1	0	0
+2	+0	+0	+8	1.102	1	0	0
4	2	0	14	1.157	1.020	0.084	0.16
6	2	2	20	1.207	1	0	0
8	6	2	24	1.219	1.035	0.148	0.35
10	8	4	28	1.228	1.032	0.133	0.26
12	8	8	32	1.237	1	0	0
14	14	8	34	1.215	1.045	0.193	0.59
16	32	26	6	0.8149	1.035	0.148	-0.61
18	32	32	8	0.8149	1	0	0
20	36	32	12	0.8373	1.022	0.089	-0.24
22	38	34	16	0.8571	1.021	0.086	-0.29
24	38	38	20	0.8745	1	0	0
26	40	38	26	0.9129	1.010	0.039	-0.20
28	40	40	32	0.9478	1	0	0
30	40	40	40	1.000	1	0	0

^a $\delta Q(\%)$ gives the percent change in Q when one restricts the deformation to axial symmetry ($\gamma_0=1$).

A brief inspection of this table shows that the deviations from axial symmetry ($\gamma_0 \neq 1$) are extremely small: when one assumes an axially symmetric deformation ($\gamma_0=1$) the resulting error in Q is always less than 1%. In fact, the zero-point fluctuations of γ are certainly at least as large as γ_0 ,²² and so an equilibrium deviation from axial symmetry cannot establish itself. We should add that most of the excited states also prefer deformations which are virtually symmetric.²³

Turning now to λ_0 as a function of the particle number A , we note (see Table I) that the first half of the shell prefers the prolate ($Q>0$), the second half the oblate ($Q<0$) shape. There is no preponderance of either positive or negative Q 's; in fact Q is roughly an odd function of A about the half-way point in the shell ($A=55$). Near the middle of the shell the lowest states with $\lambda_0>1$ and $\lambda_0<1$ are nearly degenerate, and here one can have a situation where $\gamma_0=1$ is not a stable configuration.²⁴ Except for such cases, our previous conclusion that one may put $\gamma_0=1$ will hold.

Having disposed of the complications of axial asymmetry, we now consider Q as a function of A when both protons and neutrons occupy the orbits belonging to (5). Coulomb and surface effects still being ignored. It is now convenient to define $\alpha = \alpha_x + \alpha_y$, where the sums in (9) now include both protons and neutrons. We also define α_P and β_P to be the partial sums of (9) which include only the protons, i.e.,

$$\alpha_P = \sum_{\text{protons}} (n_x^i + n_y^i + 1), \quad \beta_P = 2 \sum_{\text{protons}} (n_z^i + \frac{1}{2}). \quad (10)$$

In terms of these quantities the quadrupole moment at minimum energy is

$$Q_0^{(a)} = \frac{2}{3} Z e r_0^2 A^{\frac{2}{3}} \left(\frac{\beta_P \beta - \alpha_P \alpha}{\alpha_P \alpha + \frac{1}{2} \beta_P \beta} \right). \quad (11)$$

²² See reference 4, pp. 32-34.

²³ All formulas not given in the text will be found in Appendix I.

²⁴ D. L. Hill and J. A. Wheeler, Phys. Rev. **89**, 1102 (1953), Figs. 27 and 28; L. Wilets and M. Jean, Phys. Rev. **102**, 788 (1956).

In deriving (11), we have fixed ω by requiring the mean square radius to be $\frac{2}{3} r_0^2 A^{\frac{2}{3}}$.

Figure 1 shows how $Q_0^{(a)}$ behaves as a function of A when $Z=(2A/5)$. Roughly speaking, $115 \lesssim A \lesssim 180$ corresponds to the shell which contains the rare earths, while $A=180$ plays a role analogous to that of the doubly magic nucleus Pb^{208} . The largest $Q_0^{(a)}$ in this (115-180) "shell" is found to be 5.3 barns for $r_0=1.20 \times 10^{-13}$ cm, and 7.4 barns for $r_0=1.45 \times 10^{-13}$ cm. These values of r_0 correspond to the radii found in electron²⁵ and neutron¹⁴ scattering, respectively. The largest experimental values¹¹ for $150 \lesssim A \lesssim 180$ are approximately 9.2 barns. This very simple model, therefore, has equilibrium deformations of the correct order of magnitude for the smaller r_0 , while for the larger r_0 the agreement is quite good. Which of these radii is the correct one for this problem is open to question; the potential which would give the proper charge distribution (i.e., $r_0=1.20 \times 10^{-13}$ cm) probably would fail to reproduce the neutron-scattering data.²⁶

Though this model agrees with experiment in that it has large deformations between closed shells, we again note the approximate symmetry between the positive and negative Q 's. The model does *not* yield the preponderance of positive quadrupole moments found empirically.

We also observe that the model sometimes predicts Q to be positive just after a shell is closed ($N=40$, $N=70$, $Z=70$). In fact, the disagreement between Fig. 1 and the experimental situation¹⁶ is rather complete near the magic numbers. This result is a consequence of the high degree of degeneracy which the spectrum of the oscillator possesses at spherical symmetry ($\lambda=1$). Any small change from the oscillator shape would lift this degeneracy of states of different

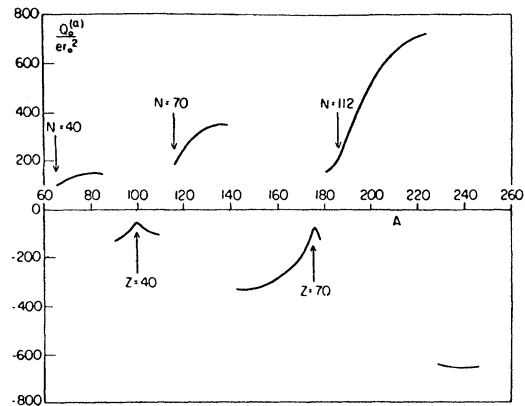


FIG. 1. Quadrupole moment as a function of A (number of particles) in an anisotropic oscillator potential. The deformation is assumed to be axially symmetric, and Coulomb repulsion and surface tension have been neglected. The arrows indicate the magic numbers for this model. $Z=0.4A$ throughout.

²⁵ K. W. Ford and D. L. Hill, *Annual Reviews of Nuclear Science* (Annual Reviews, Inc., Stanford, 1955), Vol. 5, p. 25.

²⁶ S. D. Drell, Phys. Rev. **100**, 97 (1955).

l (orbital angular momentum), and such a potential would then lead to the correct behavior in the immediate neighborhood of the magic numbers. For the large deformations which one finds between the magic numbers, such a slight reshuffling of the $(\lambda=1)$ -spectrum is of little consequence, as we shall see more clearly in Sec. III (especially Fig. 5). One should also remember that the "strong-coupling" approximation is only meaningful when the equilibrium deviation is large, and so any disagreement between our Q 's and the experimental ones is irrelevant when $\lambda_0 \approx 1$ ($Q \approx 0$).

This model also permits a comparison between the quadrupole moment of the *actual* charge distribution $Q_0^{(a)}$ and that of a *uniformly* charged spheroid whose semiaxes are $r_0 A^{1/3} \lambda_0^{-1/3}$ and $r_0 A^{1/3} \lambda_0$. This latter moment we call $Q_0^{(u)}$. Both these moments are plotted in Fig. 2, which shows that they differ by $\lesssim 15\%$ in the "strong-coupling" region ($126 \lesssim A \lesssim 166$). Naturally $Q_0^{(a)}$ is much more sensitive to the magicity of Z than $Q_0^{(u)}$ is, and conversely for N (see Fig. 2 for $A=116, 176$).

Our final task is to incorporate the effects of the Coulomb repulsion and surface tension. Since we have seen that the quadrupole moments of a uniform charge distribution approximate the exact Q very well, we assume that the Coulomb energy E_C is also well approximated by the expression appropriate to a uniformly charged spheroid. As for the surface energy $E_S(\lambda)$, we simply assume it to be proportional to the surface area of the spheroid, the proportionality factor u_s remaining variable. (According to the mass-formula, $u_s \approx 14$ Mev.)²⁷

The inclusion of E_S and E_C changes the equilibrium deformation from λ_0 to $\lambda_0(1+\kappa)$, and consequently the

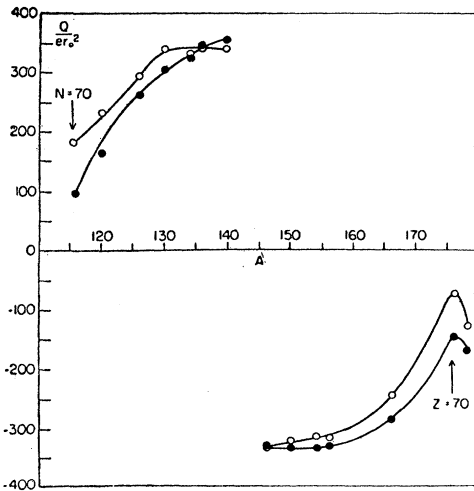


FIG. 2. Comparison of the quadrupole moments belonging to the exact charge distribution for particles moving in an anisotropic oscillator potential, and an equivalent uniform charge distribution. The open circles are the computed values of $Q_0^{(a)}$, the full circles $Q_0^{(u)}$.

²⁷ J. M. Blatt and V. F. Weisskopf, *Theoretical Nuclear Physics* (John Wiley and Sons, Inc., New York, 1952), pp. 225-233.

TABLE II. Dependence of Q on Coulomb and surface energy.

A	Z	$\left(\frac{Q_0^{(a)}}{e r_0^2}\right)$	$[Q_1^{(a)}/e r_0^2]$		
			$u_s=0$	$u_s=14$	$u_s=28$
116	46	182	186	174	163
126	50	295	304	284	275
130	52	341	354	332	309
134	54	332	345	323	301
136	54	345	359	335	311
140	56	340	355	330	306
146	58	-336	-354	-322	-289
150	60	-322	-339	-309	-278
154	62	-314	-332	-301	-271
156	62	-315	-332	-302	-272
166	66	-246	-263	-237	-213
176	70	-74	-82	-70	-58

quadrupole moment from $Q_0^{(a)}$ to some other value which we call $Q_1^{(a)}$. Table II shows $Q_1^{(a)}$ for $u_s=0, 14$, and 28 Mev. We note that the sign of $Q_1^{(a)}$ is invariably given by that of $Q_0^{(a)}$, while its magnitude differs from that of $Q_0^{(a)}$ by less than 14% for all the values of u_s considered.

The prevalence of positive Q 's has previously been accredited to the surface and Coulomb energies.²⁸ We, to the contrary, find that the approximate symmetry between $Q>0$ and $Q<0$ is completely unaltered by these effects. Our failure to explain the predominance of positive Q 's can perhaps be attributed to the fundamental shortcomings of the independent-particle model. A discussion of these shortcomings is presented at the end of Sec. III.

III. INDEPENDENT-PARTICLE MOTION IN A SPHEROIDAL POTENTIAL²⁹⁻³¹

The model investigated in the previous section does not reproduce the magic numbers correctly, ignores the spin-orbit interaction, and employs a collective potential whose shape is known to be unrealistic.¹⁴ At least the first two of these simplifications must be eliminated before one can use the model to compute such quantities as a_k or the magnetic moment.

We are therefore led to consider the motion of

²⁸ S. A. Moszkowski and C. H. Townes, *Phys. Rev.* **93**, 306 (1954). The disagreement between our conclusion and theirs is, in essence, due to the fact that these authors have, in contrast to ourselves, assumed the orbital angular momentum of a nucleon in the spheroidal potential to be conserved approximately.

²⁹ This and the following section are based on the author's doctoral thesis, Massachusetts Institute of Technology, May 16, 1955 (unpublished).

³⁰ A calculation whose objectives and methods are similar to those of this section has recently been published by S. G. Nilsson, *Kgl. Danske Videnskab. Selskab, Mat.-fys. Medd.* **29**, No. 16, (1955). Nilsson employs a collective potential of parabolic shape augmented by centrifugal and spin-orbit interactions whose strengths are chosen so that the correct magic numbers result. Although the oscillator is not as realistic a potential as we shall employ, it does admit to a much more accurate solution than we were able to obtain. The final results of the work reported here and that of Nilsson seem to be in qualitative agreement—for more details, see references 37 and 41.

³¹ S. A. Moszkowski, *Phys. Rev.* **99**, 803 (1955), has computed energy eigenvalues (though not wave functions) for particles moving in a spheroidal square well of infinite depth (see also reference 38).

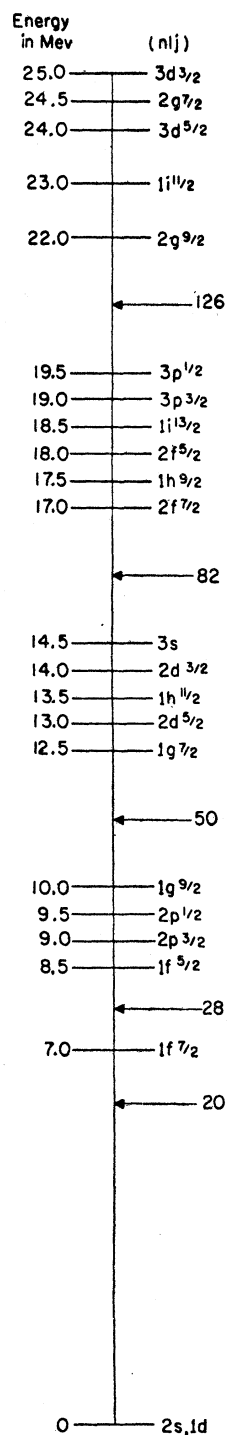


FIG. 3. Level scheme at spherical symmetry ($\lambda=1$ or $\beta=0$). These energies are called E_{nj}^w in the text (Sec. III), where $w=(-1)^l$.

course, depend on the well shape. Nevertheless, we will show (Appendix II) that for potentials which are flat over the major part of the nuclear volume and then rise to zero in a distance small compared to $r_0 A^{1/3}$, these integrals can be evaluated approximately with square well wave functions.

Our ($\lambda=1$)-scheme is very similar to Klinkenberg's¹³; it is shown in Fig. 3. The separation between levels of a given shell are arbitrarily taken as shown, and fit in roughly with the observed separations as given by the data on isomerism³² for nuclei near the magic numbers. The gaps between the major shells are taken from the experimental data³³ on such nuclei as Pb²⁰⁸. As we have already pointed out in Sec. II, and as we shall illustrate below (see Fig. 5), the details of the ($\lambda=1$)-scheme are not important in the strong-coupling region; it is only important that the levels be in the proper shells.

To each level of the ($\lambda=1$)-scheme there belong $(2j+1)$ single particle spin-orbitals $\psi_{\Omega}^w(nj)$, ($n-1$) being the number of radial nodes, j the total angular momentum of the particle, Ω the projection of \mathbf{j} on the symmetry axis, and w the parity (± 1). These wave functions are assumed to span a subspace of the Hilbert space whose basis vectors are *all* solutions of the Schrödinger equation

$$\left[T + V(r) + U(\mathbf{r}, \frac{\hbar}{i} \nabla, \mathbf{s}) - E_{nj}^w \right] \psi_{\Omega}^w(nj) = 0; (\lambda \equiv 1). \quad (12)$$

Here T is the kinetic energy, $V(r)$ is a purely central potential, and $U(\mathbf{r}, (\hbar/i) \nabla, \mathbf{s})$ represents the spin-orbit interaction, \mathbf{s} being the spin vector of the nucleon. The eigenvalues E_{nj}^w are the energies shown in Fig. 3.

We now make the further assumption that for $\lambda \neq 1$, only the potential V in the Hamiltonian of (12) changes, but not U . This simplification is motivated by the fact that U is much weaker than V .³⁴ We may then write the λ -dependent part of the Hamiltonian as

$$V(\mathbf{r}, \lambda) = V(r) + \mathfrak{W}(\mathbf{r}, \theta, \lambda), \quad (13)$$

$$V(\mathbf{r}, 1) = V(r), \quad (13')$$

θ being the azimuthal angle. The deformations described by (13) are, as always, assumed to be of the spheroidal shape. We have been unable to express \mathfrak{W} in closed form, and are therefore forced to expand it in a power series about $\lambda=1$:

$$\mathfrak{W}(\mathbf{r}, \theta, \lambda) \simeq \beta \mathfrak{W}_1(\mathbf{r}, \theta) + \frac{1}{2} \beta^2 \mathfrak{W}_2(\mathbf{r}, \theta) + \dots \quad (14)$$

Here we have introduced Bohr's β as an expansion parameter. Our λ is related to β through

$$\beta = (4\pi/45)^{1/2} \lambda^{-2} (\lambda^2 - 1). \quad (15)$$

nucleons in a collective potential which is constant ($-V_0$) throughout the interior of the nucleus, and then rises to zero quite rapidly. One may, to a limited extent, avoid a set of assumptions as to the well shape and the strength and nature of the spin-orbit force by assuming, instead, a ($\lambda=1$)-level scheme. The radial integrals required to carry out the calculation will, of

³² M. Goldhaber and R. D. Hill, Revs. Modern Phys. **24**, 179 (1952).

³³ Elliott, Graham, Walker, and Wolfson, Phys. Rev. **93**, 356 (1954). For a comprehensive compilation of such data, see G. Scharff-Goldhaber, Phys. Rev. **90**, 587 (1953).

³⁴ See, e.g., Adair, Darden, and Fields, Phys. Rev. **96**, 503 (1954).

Expressions for \mathfrak{W}_1 and \mathfrak{W}_2 will be found in Appendix II, while the consequences of retaining only quadratic terms in β are discussed at the end of this section.

We now return to the wave functions χ introduced in Sec. I. They can be written as linear combinations of the complete set defined by (12):

$$\begin{aligned}\chi_{\Omega^w}(k\beta) &= \sum_{n,j} C_{\Omega^w}(k\beta|n,j)\psi_{\Omega^w}(n,j), \\ \chi_{-\Omega^w}(k\beta) &= \sum_{n,j} (-1)^{i-\frac{1}{2}} C_{\Omega^w}(k\beta|n,j)\psi_{-\Omega^w}(n,j).\end{aligned}\quad (16)$$

The quantum number k serves the same purpose here as in Eq. (1).

The secular equation

$$\begin{aligned}\sum_{n',j'} C_{\Omega^w}(k\beta|n',j') \{ [E_{n,j^w} - E_{\Omega^w}(k;\beta)] \delta_{n,n'} \delta_{j,j'} \\ + \langle n,j|\Omega w | n',j' \Omega w \rangle \} = 0,\end{aligned}\quad (17)$$

then determines the coefficients C_{Ω} , and the energy levels $E_{\Omega^w}(k;\beta)$ in the spheroidal force field. Since the energy only depends on the absolute value of Ω , all levels are doubly degenerate.

Clearly we cannot diagonalize the infinite matrix defined by (17), and we have to confine ourselves to a finite subspace. Since we will be interested in nuclei between the magic numbers 50 and 126, we restrict ourselves to the subspace spanned by the states $\psi_{\Omega^w}(n,j)$ lying between magic number 8 and the top of the shell above 126. This subspace is just the one illustrated in Fig. 3.

The radial integrals implicit in the matrix elements of \mathfrak{W} still remain to be determined. These are the integrals which we compute with square well radial functions; the validity of this procedure is briefly discussed in Appendix II.

The eigenvalues E_{Ω} and eigenvectors C_{Ω} have been found³⁵ for six values of β ($\pm 0.2, \pm 0.3, \pm 0.4$), one well depth ($V_0 = 35$ Mev), and one radius [$R_0 = 1.45 \times (170)^{\frac{1}{3}} \times 10^{-13}$ cm]. The energy levels are shown in Fig. 4, but because of limitations of space, the coefficients C_{Ω} are not reproduced here.³⁶

A glance at Fig. 4 shows that the deformation completely destroys the shell structure of the ($\beta=0$)-scheme. As we have remarked above, the level scheme for large deformations depends only on the gross features of the ($\beta=0$)-scheme, and not its details. To illustrate this point, we have carried out the computations for a set of $|\Omega| = \frac{1}{2}$ states which are grouped into (a) completely degenerate, and (b)

separated shells, when $\beta=0$. The results are given in Fig. 5. We see that for the larger values of β ($\gtrsim 0.2$), the two sets of levels agree extremely well.

An inspection of the tables³⁶ of the C_{Ω} 's reveals that for the majority of states these quantities are rather slowly varying functions of β , once $\beta \gtrsim 0.2$. This means that a_k and the magnetic moments will not, in general, depend sensitively on β in the strong-coupling region. There are exceptions to this rule, of course; for example, $\chi_{\frac{3}{2}}^+(k=8, \beta>0)$ and $\chi_{\frac{3}{2}}^+(k=13, \beta>0)$ have very rapidly changing coefficients. This behavior is a consequence of the Wigner-von Neumann no-crossing theorem, which states that any pair of levels having the same parity and Ω cannot cross, and that their expansion coefficients will be exchanged as one passes from one side of the point of closest approach to the other.

Before we consider any applications of the levels scheme and wave functions, we must discuss the implications of the various approximations we have made. The three basic errors in the procedure outlined so far are due to (i) the deletion of a minority of the bound states (those below magic number 8) as well as the complete continuum; (ii) the truncation of \mathfrak{W} as expressed by Eq. (14); (iii) the basic assumptions listed at the end of Sec. I. We shall not discuss the latter again except as they affect (i) and (ii).

It is relatively easy to estimate the importance of the neglected bound states by simply enlarging the matrix by a few steps and repeating the diagonalization. This has been done for one case, and one finds that the quoted results are reliable, except at the top of the energy scale (see Fig. 4), where most of the levels rise to sharply and would be forced down by the states above.³⁷ Most of the nuclei with which we are concerned are found not to occupy these unreliable levels, and so we are justified in deleting some of the bound states. It is much more difficult to estimate the effect of the continuum; all we can say is that it will tend to push all the computed levels downward, i.e., add a negative term to each level roughly quadratic in β . One would expect the continuum to depress a set of neighboring states by roughly the same amount, and since only relative positions of levels are of importance, only the fluctuations of these depressions would be of consequence. We may therefore hope that the deletion of the continuum also does not introduce any appreciable errors.

³⁵ The diagonalization was carried out on Whirlwind, MIT's digital computer. We would like to thank Mr. F. J. Corbato and Dr. A. Meckler for supplying the necessary programs.

³⁶ Tables of C_{Ω} have been deposited as Document number 4881 with the ADI Auxiliary Publications Project, Photoduplication Service, Library of Congress, Washington 25, D. C. A copy may be secured by citing the Document number and by remitting \$1.25 for photoprints, or \$1.25 for 35 mm microfilm. Advance payment is required. Make checks or money orders payable to: Chief, Photoduplication Service, Library of Congress.

³⁷ B. R. Mottelson and S. G. Nilsson have also assigned spins in this region, using Nilsson's level scheme. The agreement with experiment seems to be as extensive as ours. A comparison of our level schemes show that they have many characteristics in common and differ mainly in the details of level ordering up to the middle of the 82-126 shell. Above this point (defined roughly by the Hf isotopes) we differ considerably, as is to be expected since the deletion of the continuum becomes rapidly less justifiable as the top of the discrete spectrum is reached. A more detailed comparison of our schemes will be possible when Nilsson's results concerning moments, a_k , etc., are published. [In this connection, see also B. R. Mottelson and S. G. Nilsson, *Z. Physik* 141, 217 (1955) for a discussion of Tm¹⁶⁹, and compare with our Table III.]

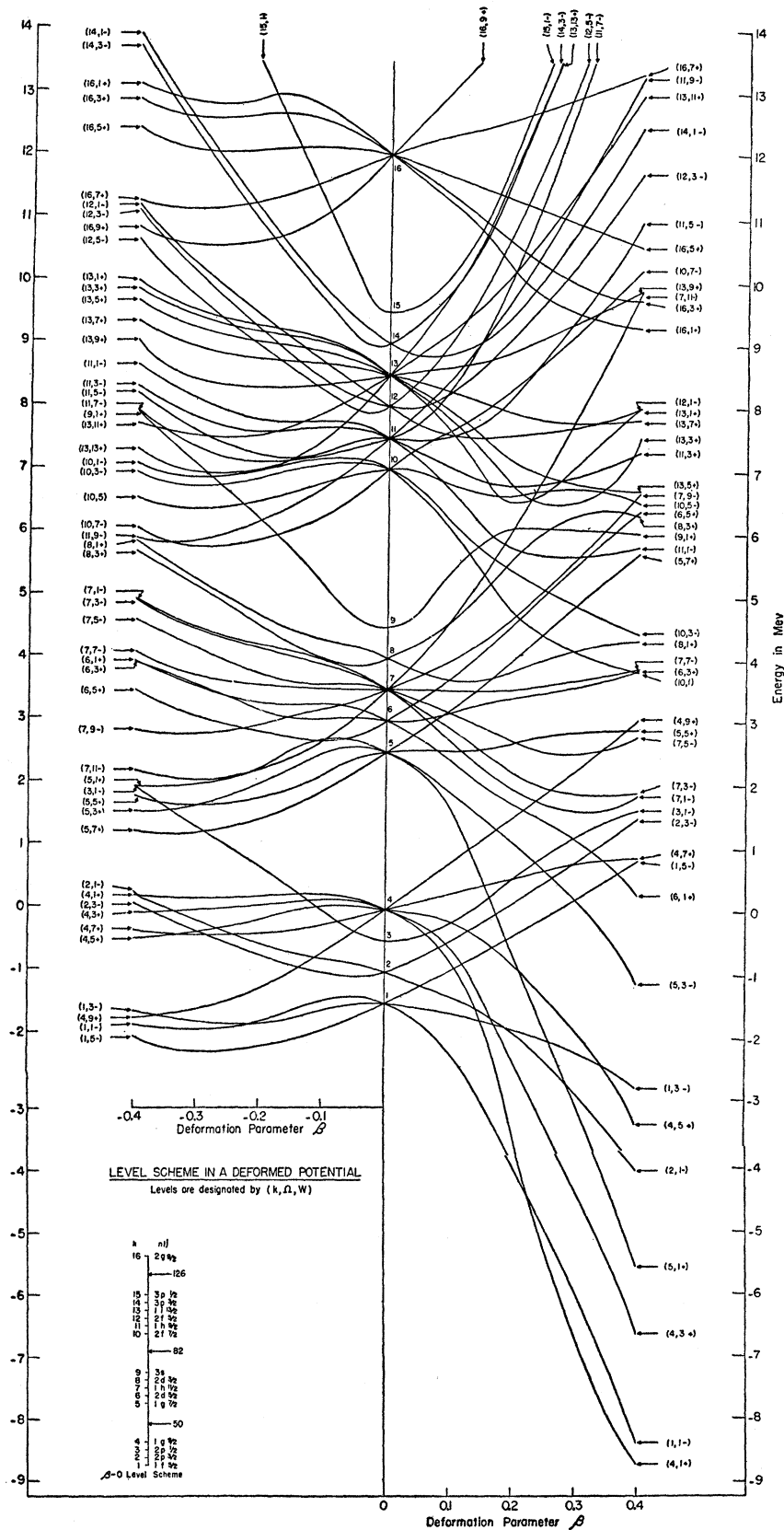


FIG. 4. Level scheme in a deformed potential. The properties of this potential are described in Sec. III. The levels are here designated by $(k, 2|\Omega, w)$. The quantum number k is defined by the position of the level as $\beta \rightarrow 0$ in the manner indicated. The lowest levels shown originate from $1f_{5/2}$, the highest from $2g_{9/2}$. The β dependences of the other levels of Fig. 3 have also been computed, but are not shown because the calculation is unreliable for $E \gtrsim 10$ Mev, $E \lesssim -7$ Mev, where E designates the energy scale of the graph. The zero of the E -scale is arbitrarily taken at the level $(\beta=0, n=1, j=9/2, w=+1)$.

As for the expansion of \mathcal{W} , there is no practical way of estimating the importance of the cubic and higher terms. In the case of the oscillator model, this expansion results in energy levels and wave functions which agree quite well with the exact solutions (see Fig. 6). On the other hand, these same approximate levels lead to a strong favoring of positive quadrupole moments. As we know, this is not true of the exact solutions.

We therefore believe that our method will give energy eigenvalues³⁸ and wave functions which are sufficiently accurate for level assignments and the computation of such quantities as a_k , the magnetic moments, and transition probabilities. Our energy levels are, unfor-

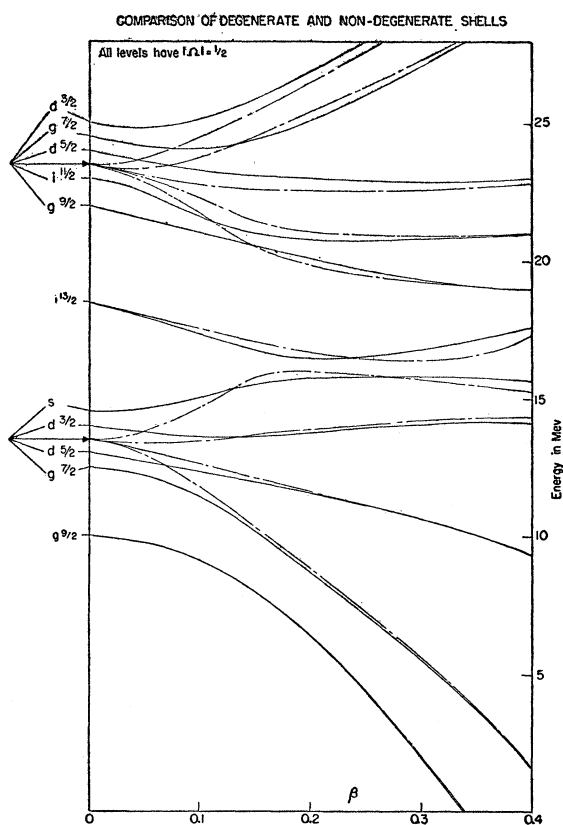


FIG. 5. Comparison of degenerate and nondegenerate shells for $|\Omega| = \frac{1}{2}$, $w = +1$. The solid curves are taken from Fig. 4. The broken curves show the levels one obtains when one assumes completely degenerate shells at $\beta = 0$. The quantum numbers of the levels when $\beta = 0$ are shown on the left.

³⁸ J. Uretsky [Ph.D. thesis, Massachusetts Institute of Technology, May, 1956 (unpublished)] has computed eigenvalues for the spheroidal square wall of finite depth, but *without* spin-orbit interaction. He finds that Moszkowski's approximation method (reference 31) yields more accurate results for energy levels than does an expansion of our type [see Eq. (14)]. Any further comparison between our work and that of Moszkowski is difficult, since he has not computed wave functions and therefore cannot determine many quantities such as the magnetic moments. As for the equilibrium deformations, Moszkowski's calculations do not extend into the heavy-element region. Because of the deletion of the spin-orbit coupling, Uretsky's results can also not be compared directly with ours, nor with the experimental data.

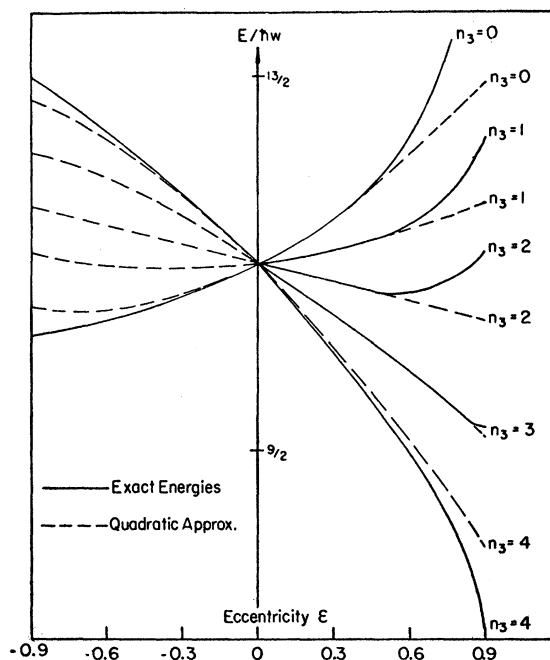


FIG. 6. Comparison of exact and approximate levels in a deformed oscillator potential ($N=4$) shell. The approximation corresponds to an expansion in powers of β up to and including quadratic terms.

tunately, too crude to determine the equilibrium deformation β_0 and the associated quadrupole moment.

This failure to predict β_0 is seen in a somewhat better light³⁹ if one remembers that the determination of the equilibrium deformation is, in essence, dependent upon a knowledge of the total binding energy as a function of β . That such knowledge cannot be extracted from the independent particle model is well known. Let us briefly review the reasons for this last observation, and rephrase the argument for our purposes.⁴⁰ If we assume that the spherically symmetric potential $V(r)$ which appears in Eqs. (12) and (13') is the result of a Hartree-Fock calculation, we have implicitly assumed that the spatial dependence of the fundamental nuclear forces are such as to lead to weak correlations (little particle clustering). For the sake of argument, let us agree that this implicit assumption is justified. When we deform $V(r)$ as previously outlined, the resultant potential $V(r, \lambda)$ is not self-consistent, even if $V(r)$ was. That is to say, the value of β_0 determined in the naive fashion of Sec. II will not necessarily minimize the expectation value of the many-body Hamiltonian with our states χ as trial functions. We should also note that the inclusion of a surface tension is merely a symptom of the lack of

³⁹ We should point out that the levels of Fig. 4 do lead to large equilibrium deformations between the magic numbers. They are too crude to reliably determine β_0 's actual value or sign, but are completely consistent with the fact that $0.2 \lesssim \beta \lesssim 0.4$ for the nuclei of interest.

⁴⁰ See reference 27, pp. 278-292. K. A. Brueckner, Phys. Rev. 100, 36 (1955).

self-consistency: a truly self-consistent procedure would automatically account for the depletion of bonding as the surface area is increased. It is to be expected that a classical surface tension can, to a certain extent, compensate for the lack of self-consistency.

Even if we ignore all the fundamental shortcomings of our method, and boldly assume that $V(\mathbf{r}, \lambda)$ is the self-consistent potential for an A -body system interacting through two-body forces, our computational difficulties are still not resolved. For, as we had seen in Sec. II,²¹ in addition to the energy levels, one must also know the expectation value of $V(\mathbf{r}, \lambda)$ in all the states χ . The evaluation of these expectation values is a formidable computational task which we have not undertaken. Finally, a proper calculation of Q as a function of A would require a set of level schemes such as the one of Fig. 4 for a variety of nuclear radii.⁴¹

The shell model scheme is employed only as a guide in assigning spins and estimating magnetic moments and decay probabilities. It is not intended for computing binding energies. Our scheme has similar limitations. It does not claim an essentially broader area of applicability than the shell model does, and is to be treated as a replacement of the latter whenever the deviations from spherical shape are large.

IV. GROUND-STATE SPINS AND MAGNETIC MOMENTS

In the strong-coupling limit, and with the assumption of independent-particle motion in the deformed potential, the spin, parity, and magnetic moment of nuclear states are easily determined. For even-even nuclei, the ground state has spin zero and even parity, since all levels are degenerate in $\pm\Omega$, and filled pair-wise. The magnetic moment, spin, and parity of the ground state of odd- A nuclei are completely determined by the odd nucleon. The parity is that of the level occupied by the odd particle, and the spin I_0 equals the Ω value of this level, unless $|\Omega| = \frac{1}{2}$, in which case I_0 depends on a_k .¹⁰ The matrix element which defines a_k [see Eq. (4)] is readily evaluated in terms of our wave functions χ . One finds that⁴²

$$a_k = \sum_{nj} (-1)^{j-\frac{1}{2}} (j + \frac{1}{2}) |C_{\frac{1}{2}}^w(k\beta | nj)|^2. \quad (18)$$

Under the assumptions stated above, the magnetic moment is given by the expectation value of the operator

$$\mu_{op} = g_C N_{z'} + g_l l_{z'} + g_s s_{z'} \quad (19)$$

in the strong-coupling state (1) with $M=I$. In (19) $N_{z'}$, $l_{z'}$, and $s_{z'}$ are the projections of the collective, odd-particle orbital, and odd-particle spin angular momenta on the *space*-fixed z' -axis, respectively. g_C is the g -factor for the collective rotation and is presumably of order Z/A (≈ 0.4), although there is some evidence that g_C might be smaller than this.⁴² The other g -factors have their usual meaning: $g_l=0$ or 1, $g_s=-3.83$ or 5.59, depending on whether the odd nucleon is a neutron or proton, respectively. We may eliminate $N_{z'}$ and $l_{z'}$ from (19), and write the magnetic moment as

$$\mu = g_C I + (g_l - g_C) \langle j_{z'} \rangle_{M=I} + (g_s - g_l) \langle s_{z'} \rangle_{M=I}. \quad (20)$$

The expectation values appearing in (20) have been evaluated elsewhere,^{29,30} and are listed in Appendix III.

One of the interesting properties of the strong-coupling magnetic moments is that they always lie inside the Schmidt lines.⁵ Another most striking feature of these moments is that they do not have the simple connection with the parity that the shell model moments do. This is immediately understood if one recalls that our state χ is composed of orbitals $\psi_{\alpha^w}(nj)$ belonging to opposite Schmidt lines. From this it follows that in the regions of strong deformation the proximity of the magnetic moment to the Schmidt lines does not determine the parity of the nuclear ground state. This fact makes the determination of the absolute parity of nuclear states very difficult (see Appendix III).

We have assigned spins and parities to the nuclei in the region $150 \leq A \leq 190$ by filling our level scheme (Fig. 4) with the required number of particles, and noting the quantum numbers of the level occupied by the odd nucleon.³⁷ The magnetic numbers are then computed with the coefficients C_Ω , as are the quantities a_k . The results are collected in Table III.

The assigned level is not always the very lowest state according to the detailed scheme of Fig. 4, but might be either a level just above, or below the obvious assignment. This is done, admittedly, to improve the agreement with experiment. One attempts to justify this by arguing that the detailed ordering of levels in our scheme is not completely reliable, while the coefficients C_Ω should be more trustworthy. This can be seen by referring to Fig. 5, which shows that the details of the assumed level scheme (Fig. 3) have only small effects on a set of levels having one particular value of $|\Omega|$, and that these levels are well separated for large β . The relative positions of levels with different $|\Omega|$ are not so independent of the detailed assumptions. We also noted that the coefficients C_Ω are, with only a few exceptions, qualitatively independent of β , and so the C_Ω 's are expected to be fairly insensitive to the detailed assumptions.

In Table III we have graded the assignment as "excellent" when the level assigned is determined by a literal interpretation of our level scheme—i.e., the

⁴¹ Nilsson's model (reference 30) has a great advantage in that one may easily compute the spectrum as a function of A (i.e., radius). The greater accuracy of his solution has enabled B. R. Mottelson and S. G. Nilsson [Phys. Rev. **99**, 1615 (1955)] to compute the equilibrium deformation as a function of A , the agreement with the experimental data being excellent. One should remember, however, that the fundamental difficulty (i.e., lack of self-consistency) which we have discussed is common to all existing calculations.

⁴² A. Bohr, *Rotational States of Atomic Nuclei*, doctoral thesis (E. Munksgaars Forlag, Copenhagen, 1954).

TABLE III. Spins and magnetic moments.^a

Nucleus	Odd-part.	Assignment ($k, \Omega $) β	Remark	I_{obs}	$(I, w)_{\text{th}}$	μ_{obs}	(i)	(ii) μ_{th}	(iii)	(iv)
Eu ¹⁵¹	Z=63	(7,5/2) 0.2	exc. b	5/2	(5/2)−	3.4	3.15	3.00	2.90	2.74
Eu ¹⁵³	63	(5,5/2) 0.4	exc. b,c	5/2	(5/2)+	1.5	0.69	0.86	0.43	0.60
Tb ¹⁵⁹	65	(6,3/2)	exc.	3/2	(3/2)+	1.5±0.4	2.34	2.19	2.35	2.20
Ho ¹⁶⁵	67	(7,7/2)	exc.	7/2	(7/2)−	?				
Tm ¹⁶⁹	69	(8,1/2) 0.4	exc. d	1/2	(1/2)+	−0.2	−0.32	−0.25	−0.39	−0.32
Lu ¹⁷⁵	71	(7,7/2) 0.4	good	7/2	(7/2)−	2.9±0.5	4.5	4.3	4.3	4.2
Ta ¹⁸¹	73	(5,7/2) 0.4	exc. f	7/2	(7/2)+	2.1	1.46	1.66	1.30	1.50
Re ¹⁸⁵	75	(6,5/2) 0.2	exc. b	5/2	(5/2)+	3.17	3.22	3.07	2.96	2.81
Re ¹⁸⁷	75	(6,5/2) 0.2	exc. b	5/2	(5/2)+	3.20	3.22	3.07	2.96	2.81
Ir ^{191,3}	77	(10,3/2) 0.2	exc. b	3/2	(3/2)−	0.2	0.69	0.74	0.47	0.52
Gd ¹⁵⁵	N=91	(8,3/2) 0.4*	good g	3/2	(3/2)+	−0.3	−0.07	−0.07	−0.16	−0.13
Gd ¹⁵⁷	93	(11,3/2) 0.4	good	3/2	(3/2)−	−0.4	−0.71	−0.61	−0.81	−0.71
Er ¹⁶⁷	99	(13,7/2) 0.4	exc.	7/2	(7/2)+	−0.5	−0.95	−0.83	−1.07	−0.95
Yb ¹⁷¹	101	(12,1/2) 0.3	exc. h	1/2	(1/2)−	0.45	0.62	0.52	0.63	0.56
Yb ¹⁷³	103	(11,5/2) 0.3	exc.	5/2	(5/2)−	−0.66	−0.87	−0.76	−0.97	−0.86
Hf ¹⁷⁷	105	(10,7/2)	exc. i	7/2	(7/2)−	?				
Hf ¹⁷⁹	107	(13,9/2)	exc. j	9/2	(9/2)+	?				
W ¹⁸³	109	?	e	1/2	? +	0.09		?		
Os ¹⁸⁹	113	(14,1/2) 0.2	exc. b,k	1/2	(1/2)−	0.71	0.82	0.76	0.76	0.69
Pd ¹⁰⁵	59	(7,5/2) 0.2	exc. l	5/2	(5/2)−	−0.57	−0.64	−0.55	−0.74	−0.65
Ag ¹⁰⁹	Z=47	(3,1/2) 0.2*	good m,l	1/2	(1/2)−	−0.13	−0.33	−0.24	−0.37	−0.28

^a The theoretical magnetic moments correspond to the following variety of g -factors: (i) $g_C=0.40$, g_s unquenched; (ii) $g_C=0.40$, g_s quenched 10%; (iii) $g_C=0.25$, g_s unquenched; (iv) $g_C=0.25$, g_s quenched 10%. The asterisk (*) after an assignment indicates that the state in question has coefficients C_0 which are sensitive to variations of β . For a compilation of experimental spins and moments see R. J. Blin-Stoyle, *Revs. Modern Phys.* **28**, 75 (1956).

^b See reference 43.

^c This nucleus has states of intrinsic excitation at 97 keV and 103 keV; the first decays to ground via $E1$, the second via $M1$ radiation [N. Marty, *Compt. rend.* **238**, 2516 (1954)]. The first of these excited states could correspond to our orbit $(7,7/2, -)$, the second to $(6,3/2, +)$.

^d The observed value of $a_k = -0.74$, while we obtain -0.56 . For a detailed discussion of this nucleus see B. R. Mottelson and S. G. Nilsson, *Z. Physik* **141**, 217 (1955).

^e If one uses Eq. (C6) of Appendix III, one finds that the observed values of a_k and μ are not compatible with $w = -1$. One should note, however, that this nucleus has a rotational spectrum which does not obey Eqs. (2) and (3) (Sec. I) even when corrections for the rotation-vibration interaction have been applied. A. K. Kerman [Kgl. Danske Videnskab. Selskab, *Mat.-Fys. Medd.* **30**, No. 15 (1956)] has successfully interpreted this as an effect of a rotational perturbation which destroys the constancy of Ω . The spectrum of W^{183} is such that this perturbation will not change the ground state moment, but it will alter a_k and its relationship with μ .

^f Excited states with $I = \frac{1}{2}$ (612 keV) and $I = 5/2$ (480 keV) have been observed (see Alaga *et al.*). Our scheme does not provide for an $(I = \frac{1}{2})$ -state in this region, since a_k for both $(9,1/2, +)$ and $(11,1/2, -)$ is such that $I \neq \Omega$. On the other hand, the decay scheme is not completely understood, since the 612-keV level has two unresolved components [R. V. Pound and A. Sunyar (private communications)].

^g Gd^{155} has two nucleonic excited states at 86 keV and 105 keV, both of which go to ground via $E1$ transitions [E. L. Church, *Bull. Am. Phys. Soc. Ser. II*, **1**, 180 (1956)]. One of these could be the incorrectly assigned $\Omega = 3/2$ level, the other any of the orbits $(13,5/2, +)$, $(13,1/2, +)$ or $(12,1/2, -)$.

^h The theoretical value of $a_k = 1.2$.

ⁱ The experimental level scheme [Marmier, Boehm, and DuMond, *Phys. Rev.* **98**, 280(A) (1955)] indicates that the ground state has $I_0 = 7/2$; this is confirmed by the recent spectroscopic measurements of D. R. Speck and F. A. Jenkins, *Phys. Rev.* **101**, 1831 (1956). There is an intrinsic excitation at 320 keV which is tentatively assigned as $I = 9/2$, with opposite parity to that of the ground state. This excited state would correspond to our orbital $(13,9/2, +)$ which lies just above $(10,7/2, -)$ in Fig. 4. For a discussion of the magnetic moment, see footnote j.

^j The spin of Hf^{179} has also been determined by D. R. Speck and F. A. Jenkins, *Phys. Rev.* **101**, 1831 (1956). Furthermore, they find that $R = \mu(Hf^{177})/\mu(Hf^{179}) = -1.28$. With the assignments as shown, we find that $R_{\text{theo}} = -1.47$. The theoretical moments which lead to this are $\mu(177) = 1.56$, $\mu(179) = -1.06$, for $g_C = 0.40$, g_s unquenched.

^k The theoretical value of $a_k = -0.35$.

^l The strong-coupling approximation is probably not valid for this nucleus.

^m The experimental information concerning this nucleus will be found in Alaga, Alder, Bohr, and Mottelson, *Kgl. Danske Videnskab. Selskab. Mat.-Fys. Medd.* **29**, No. 9 (1955). If one interprets the levels observed in Coulomb excitation as a rotational band, one finds that $a_k(\text{obs}) = 0.67$, while the theoretical value is 0.65. There is also an excited nucleonic state at 88 keV which decays by emitting $E3$ radiation. This level would be our state $(4,7/2, +)$ which is seen to lie just above $(3,1/2, -)$ for $\beta \approx 0.2$. The $E1$ transition from the 400-keV rotational state to this $(7/2, +)$ -state is 10^6 times slower than the single-particle estimate. This is partially due to K -forbiddenness, but can also be attributed to the fact that our state $(4,7/2, +)$ is almost a pure (96%) $(j = 9/2)$ -state, while the ground state has only 1% of $(j = 9/2)$ and $(j = 7/2)$ in it. There is therefore a very important suppression of the nucleonic $E1$ matrix element. As for the isomeric transition, the suppression is not nearly so drastic, since about 20% of the ground state can be connected to the $(7/2, +)$ -state by the $E3$ operator.

detailed ordering of Fig. 4 is taken at face value. There is only one qualification here, which is that we put assignments under the "excellent" category when the higher of two levels which cross each other is occupied first, as for example the pair of orbits $(5,5/2, +)$ and $(7,5/2, -)$. This is justified since we do not expect our calculation to give us the exact crossing point, and also because we do not know β too well from the experimental data. When one has to go somewhat astray to attain a reasonable assignment, the grading is "good." Thus the "excellent" assignment for Lu^{175} would be $(8,1/2, +)$ or $(10,3/2, -)$, while the assignment which has the correct spin is $(5,7/2, +)$ and is termed "good."

In the strong-coupling region⁴³ there are fifteen

⁴³ The lower limit of this region is quite well defined by $Sm^{150,152}$ [G. Scharff-Goldhaber and J. Weneser, *Phys. Rev.* **98**, 212 (1955)]. The upper limit is somewhat ambiguous but appears to lie between W^{183} [Murray, Boehm, Marmier, and DuMond,

odd- A nuclei whose spin is known, and we are able to assign eleven in the category "excellent," three in "good," and for one (W^{183}) no level which has the correct spin and a reasonable value of μ or a_k is available.

In addition to assigning spins, we have also computed μ for these nuclei. The agreement between theory and experiment is more limited here. This was to be expected since μ is sensitive to the structure of the wave function χ_Ω . We thus find serious disagreement between μ_{th} and μ_{obs} for Eu^{153} , Lu^{175} , and of course W^{183} . In some other cases, the value of μ_{th} leaves something to be desired. Nevertheless, there are a number of important successes. Thus the great difference between the moments of the two europium isotopes is reproduced,

Phys. Rev. **97**, 1007 (1955)] and Os^{186} [Johns, McMullen, Williams, and Nablo, *Can. J. Phys.* **34**, 69 (1956)]. The data of the last reference would appear to indicate that the strong-coupling approximation is not valid for Re^{185} .

a fact that the shell model is unable to explain.⁴⁴ There is also reasonably good agreement between theory and experiment for both a_k and μ in Tm¹⁶⁹ (see footnote *d* of Table III).

Besides these nuclei which are almost certainly in the strong-coupling region, there are a small number of examples which may lie outside that region. For three nuclei of this latter class (Re^{185,187}, Os¹⁸⁹), "excellent" assignments which lead to extremely good values of μ_{th} are available. For the Ir isotopes an "excellent" spin assignment is also possible.

The spins and moments for two lighter nuclei (Pd¹⁰⁵, Ag¹⁸⁹) have also been evaluated, and are listed in Table III. The strong-coupling approximation is probably not applicable to these nuclei, since the quadrupole moments found in their neighborhood are not sufficiently large.

Lastly, we have calculated these moments not only with $g_c = (Z/A) = 0.40$ and the free-space g_s -factors, but also with $g_c = 0.25$ and 10% quenched nucleon g -factors.⁴⁵ The results are given in the last three columns of Table III. These changes in the g -factors effect the value of μ slightly, but it is difficult to discern any systematic improvement due to such alterations. It would appear that there is a very doubtful improvement with $g_c = 0.40$ and g_s 10% quenched. This should not be taken too seriously, however, since $(\mu_{obs} - \mu_{th})$ is often much greater than $(\mu_{th} - \mu'_{th})$.

We believe that the spin assignments based on our level scheme are much more successful and effortless than those of the shell model.¹³ In the latter there are simply too many states of high spin in this region of the isotope chart, and so one must resort to rather unconvincing level assignments to obtain the very large number of low spins demanded by the data. In the strong-coupling approximation, on the other hand, the majority of states will necessarily have low spins, since every state of the $\beta = 0$ scheme has a substate with $\Omega = \frac{1}{2}$, etc.

One should note that our scheme invariably assigns the correct spin for $63 \leq Z \leq 77$ (except for $Z = 71$, which falls under "good"), and similarly for $99 \leq N \leq 105$. For $N = 107$ we have the important flaw of W¹⁸³,⁴⁶ which is probably due to the fact that our calculation should be quite unreliable for states near the top of the well.³⁷ To summarize the information contained in Table III, we would therefore say that our scheme must be essentially correct for the strongly deformed nuclei whose odd particles lie in the 50–82 shell or the lower part of the 82–126 shell.

Finally, we should remember that the assumption of completely independent particle motion is a rather drastic simplification. The nucleon mean free path as

deduced from the optical model¹⁴ indicates that the residual interactions are by no means negligible, though considerably smaller than one thought them to be before the advent of the shell model. One might hope that the inclusion of internucleon forces would not be too important for the determination of the essential features of the level scheme of Fig. 4, but they would undoubtedly effect the wave functions and therefore the magnetic moments.

The author takes great pleasure in acknowledging the helpful guidance, friendly interest, and constructive criticism with which Professor Victor Weisskopf has always been so liberal. He is indebted to Professor Felix Villars for numerous discussions concerning all facets of this problem, and to Professor Aage Bohr for a very informative conversation during the early stages of the work. Dr. E. Church, Dr. A. Sunyar, and Dr. M. Goldhaber kindly brought some of the experimental information discussed in Table III to the author's attention.

APPENDIX I

The particle energy $E_P(\gamma, \lambda)$ [see Eq. (8)] is minimized for

$$\gamma = (\alpha_y / \alpha_x)^{\frac{1}{2}} \equiv \gamma_0; \quad \lambda = [\frac{1}{2} \mathfrak{B} (\alpha_x \alpha_y)^{-\frac{1}{2}}]^{\frac{1}{2}} \equiv \lambda_0, \quad (A1)$$

and the corresponding value of E_P is

$$E_P(\gamma_0, \lambda_0) = (9/4) 2^{-\frac{1}{2}} \hbar \omega (\alpha_x \alpha_y \mathfrak{B})^{\frac{1}{2}}. \quad (A2)$$

For each value of A one must determine which levels should be occupied so as to get the lowest possible minimum energy. The solution of this problem is greatly facilitated if one studies the equilibrium energy $E_P(\gamma_0, \lambda_0)$ as a function of α_x , α_y , and \mathfrak{B} , and not the original expression (8).

Let us now consider the three-parameter symbol $(\alpha_x, \alpha_y, \mathfrak{B})$ which characterizes each state. If (for fixed A) two states have symbols which differ only by a permutation of the three entries, the states are identical and should not be counted as two distinct states. This remark follows from the observation that two such states differ only by a redefinition of the x , y , or z axis in the rotating coordinate system, and are therefore one and the same physical state.

We assume that we have completely filled the orbitals belonging to the shells $N = 0, 1, 2, \dots, k-1$ with pairs of particles. The total number of particles is then

$$A_{k-1} = \sum_{s=0}^{k-1} (s+1)(s+2).$$

We now proceed to fill the shell $N = k$. It then follows from (A2) that for any $A < A_k$ the lowest state is realized when only orbits belonging to the shell $N = k$ are occupied. That is to say, by raising particles to higher shells ($N > k$) we always construct an excited state. This means that if one is only interested in the ground state, α_x , α_y , and \mathfrak{B} are not independent variables, since for all occupations that have to be

⁴⁴ A. Arima and H. Horie, Progr. Theoret. Phys. (Japan) **12**, 623 (1954).

⁴⁵ F. Bloch, Phys. Rev. **83**, 839 (1951); A. de Shalit, Helv. Phys. Acta **24**, 296 (1951).

⁴⁶ A detailed investigation of this nucleus has been made by A. K. Kerman, Kgl. Danske Videnskab. Selskab, Mat.-fys. Medd. **30**, No. 15 (1956).

considered,

$$\alpha_x + \alpha_y + \frac{1}{2}\beta = \mathcal{C} = \sum_{i=1}^A (N^i + \frac{3}{2}).$$

Evidently \mathcal{C} depends only on A and not on the quantum numbers n_x, n_y, n_z of the last occupied levels.

It will now be convenient to introduce new variables η and ξ by

$$\mathcal{C}\xi = \alpha_y - \alpha_x, \quad \mathcal{C}\eta = \frac{1}{2}\beta - \frac{1}{2}\mathcal{C},$$

in terms of which (A2) becomes

$$\eta^2 + \frac{1}{3}\xi^2 + \eta(\xi^2 - \eta^2) = \mathcal{R}^2, \quad (\text{A3})$$

with

$$\mathcal{R}^2 = (4/27) - \frac{1}{2}(8E_F/9\mathcal{C}\hbar\omega)^3.$$

Since $|\eta|, |\xi| \ll 1$, (A3) is approximately an ellipse. The larger the semiaxes $(\mathcal{R}, \sqrt{3}\mathcal{R})$, the lower is the energy. It is then a simple matter to compute \mathcal{R} for each possible state of A particles; the state with largest \mathcal{R} is the ground state. The results quoted in Table I were obtained in this way.

Having determined (γ_0, λ_0) , one then computes the quadrupole moment by assuming the charge Ze to be uniformly distributed throughout an ellipsoid whose semiaxes are $(R\gamma_0^{-1}\lambda_0^{-\frac{1}{2}}, R\gamma_0\lambda_0^{-\frac{1}{2}}, R\lambda_0)$. This moment is given by⁴⁷

$$Q = \frac{2}{5}ZeR^2(\gamma_0^4\lambda_0)^{-1}[(\lambda_0^3 - \gamma_0^2) + (\gamma_0^4 - 1)(\lambda_0^3 - \frac{1}{2}\gamma_0^2)],$$

which, for small deviations from axial symmetry, is well approximated by

$$Q \simeq \frac{2}{5}ZeR^2\lambda_0^{-1}[(\lambda_0^3 - 1) - \frac{1}{8}\mathcal{E}_{xy}^4 + \dots]. \quad (\text{A4})$$

Here, as before, $\mathcal{E}_{xy}^2 = \gamma_0^4 - 1$. The last column of Table I is computed from (A4).

With the restriction to cylindrical symmetry ($\gamma_0 \equiv 1$), the equilibrium value of λ becomes

$$\lambda_0 = (\beta/\alpha)^{\frac{1}{2}}, \quad (\alpha \equiv \alpha_x + \alpha_y), \quad (\text{A5})$$

and the corresponding energy is

$$E_F(\lambda_0) = (9/8)\hbar\omega(\alpha^2\beta)^{\frac{1}{2}}. \quad (\text{A6})$$

The most advantageous level occupations are obtained if one adheres to the simple rule that for $\lambda > 1$ states of highest n_z are filled first, and vice versa for $\lambda < 1$.

The quadrupole moment of the charge distribution belonging to the wave function is

$$\begin{aligned} Q_0^{(a)} &= e \sum_{i=1}^Z \langle 2z_i^2 - x_i^2 - y_i^2 \rangle_i \\ &= e(\hbar/m\omega)\lambda_0^{-\frac{1}{2}}(\beta_P\lambda_0^{\frac{1}{2}} - \alpha_P). \end{aligned} \quad (\text{A7})$$

The requirement that the mean square charge radius is given by $\frac{2}{5}r_0^2A^{\frac{1}{3}}$ determines $\hbar\omega$ to be

$$\hbar\omega = (5/3)mc^2(\lambda_N/r_0)^2A^{-\frac{1}{3}}Z^{-1}(\alpha^2\beta)^{-\frac{1}{2}} \times (\alpha_P\alpha + \frac{1}{2}\beta_P\beta), \quad (\text{A8})$$

⁴⁷ Perhaps we should point out that this and all other formulas given in this paper for Q refer to the quadrupole moment of the charge distribution as seen in the rotating frame. The relationship between our Q 's and the spectroscopically observed value is $Q_{\text{obs}} = [3K^2 - I(I+1)]I(I+1)(2I+3)^{-1}Q$.

where λ_N is the Compton wavelength of the nucleon. If we now substitute (A5,8) into (A7), we find the expression for $Q_0^{(a)}$ given in the text.

The other quadrupole moment $Q_0^{(u)}$ defined in the text is obtained directly from (A4,5) with $\mathcal{E}_{xy} = 0$, $R = r_0A^{\frac{1}{3}}$:

$$Q_0^{(u)} = \frac{2}{5}er_0^2A^{\frac{1}{3}}Z(\alpha^2\beta)^{-\frac{1}{2}}(\beta^2 - \alpha^2). \quad (\text{A9})$$

The surface energy is given by

$$E_S(\lambda) = \frac{1}{2}u_SA^{\frac{1}{3}}\left[\lambda^{-1} + \epsilon^{-1}\lambda^{\frac{1}{2}} \times \begin{cases} \sin^{-1}\epsilon & (\lambda > 1) \\ \sinh^{-1}\epsilon & (\lambda < 1) \end{cases}\right], \quad (\text{A10})$$

where the eccentricity ϵ is defined by

$$\epsilon = +[\lambda^{-2}(\lambda^3 - 1)]^{\frac{1}{2}}.$$

The Coulomb energy for a uniformly charged spheroid is⁴⁸

$$E_C(\lambda) = E_C^0(\lambda\epsilon)^{-1} \times \begin{cases} \frac{1}{2} \ln(1+\epsilon)(1-\epsilon)^{-1} & (\lambda > 1) \\ \tan^{-1}\epsilon & (\lambda < 1) \end{cases}, \quad (\text{A11})$$

$$E_C^0 = (3Z^2e^2/5r_0A^{\frac{1}{3}}).$$

When we add E_S and E_C to the particle energy, the equilibrium point is shifted from λ_0 to $\lambda_0(1+\kappa)$. For $|\kappa| \ll 1$, we find that

$$\kappa \simeq \frac{8}{3\beta\hbar\omega} [E_C^0\Gamma_C(\lambda_0) - \frac{1}{6}u_SA^{\frac{1}{3}}\Gamma_S(\lambda_0)], \quad (\text{A12})$$

with

$$\Gamma_C(\lambda) = -\sigma^{-1} + \left(\frac{2\lambda^3\sigma + 3}{2\lambda^3\sigma\epsilon} \right) \times \begin{cases} \frac{1}{2} \ln \frac{1+\epsilon}{1-\epsilon} & (\lambda > 1) \\ \tan^{-1}\epsilon & (\lambda < 1) \end{cases},$$

$$\Gamma_S(\lambda) = \sigma^{-1}(3-2\sigma) + \left(\frac{\lambda^3\sigma - 3}{\lambda^3\sigma\epsilon} \right) \times \begin{cases} \sin^{-1}\epsilon & (\lambda > 1) \\ \sinh^{-1}\epsilon & (\lambda < 1) \end{cases},$$

and

$$\sigma = \lambda^{-2}(\lambda^3 - 1). \quad (\text{A13})$$

The approximate expression (A12) is adequate since we find that $|\kappa| \lesssim 4 \times 10^{-2}$ for $u_S \lesssim 28$ Mev.

The total energy at equilibrium is

$$\begin{aligned} E_T(\lambda_1) &= E_P(\lambda_1) + E_S(\lambda_1) + E_C(\lambda_1) \quad [\lambda_1 = \lambda_0(1+\kappa)] \\ &\simeq (1 - \frac{1}{4}\kappa^2)E_P(\lambda_0) + E_S(\lambda_0) + E_C(\lambda_0). \end{aligned} \quad (\text{A14})$$

The factor $(1 - \frac{1}{4}\kappa^2)$ preceding $E_P(\lambda_0)$ in (A14) must be taken into account. Its neglect leads to the erroneous conclusion that E_S tends to favor positive quadrupole moments. One must also use the closed expressions (A10,11) for E_S and E_C ; for the values of λ considered, the expansions in powers of σ are inadequate.

The correction to $Q_0^{(a)}$ due to the shift $\lambda_0 \rightarrow \lambda_1$ is found by simply replacing λ_0 by $\lambda_0(1+\kappa)$ in (A7). We obtain

$$Q_1^{(a)} = Q_0^{(a)} \left[1 + \kappa \left(\frac{\beta_P\beta + \frac{1}{2}\alpha_P\alpha}{\beta_P\beta - \alpha_P\alpha} \right) + O(\kappa^2) \right]. \quad (\text{A15})$$

⁴⁸ See, e.g., K. Woeste, Z. Physik 141, 643 (1955).

APPENDIX II

The potential $V(\mathbf{r}, \lambda)$ can be rewritten as

$$V(\mathbf{r}, \lambda) = V[r(1-\sigma)^{-1/6}(1-\sigma \cos^2 \theta)^{1/2}], \quad (\text{B1})$$

where σ is defined by (A13). By expanding (B1) in powers of σ , we find that

$$\mathcal{W}_1(r, \theta) = -Y_{20}(\theta)rV'(r), \quad (\text{B2})$$

$$\mathcal{W}_2(r, \theta) = (5/4\pi)[1 - 2(4\pi/5)^{1/2}Y_{20}(\theta)]rV'(r) + [Y_{20}(\theta)]^2[r^2V''(r) - rV'(r)], \quad (\text{B3})$$

where Y_{20} is a normalized spherical harmonic, and primes indicate differentiations with respect to the argument. If $V(r)$ is assumed to be a square well, the required radial integrals are

$$\langle nl|rV'(r)|n'l'\rangle = 2V_0K_{nl}K_{n'l'} \quad (\text{B4})$$

$$= -(5 + F_{nl} + F_{n'l'})^{-1} \langle nl|r^2V''(r) - rV'(r)|n'l'\rangle, \quad (\text{B5})$$

where F_{nl} is the logarithmic derivative of the radial function on the nuclear surface, and the K_{nl} are readily expressed in terms of Hankel and Bessel functions.²⁹ The quantity K_{nl} is found to vary smoothly and slowly as a function of binding energy in the well, and to depend only slightly on the well depth and the quantum numbers. It is plotted in Fig. 7 for two values of V_0 . The simple dependence of K_{nl} on the binding energy is readily understood in terms of the virial theorem:

$$\langle rV'(r) \rangle = 2\langle T \rangle, \quad (\text{B6})$$

or

$$|K_{nl}| = [\langle T \rangle_{nl} V_0^{-1}]^{1/2}. \quad (\text{B7})$$

Equation (B6) holds for any well shape; the relation

$$\langle nl|rV'(r)|n'l'\rangle = 2(-1)^{n-n'}[\langle T \rangle_{nl}\langle T \rangle_{n'l'}]^{1/2}, \quad (\text{B8})$$

which follows from (B4,7), is only rigorously true for the square well. If we could show that (B8) holds to a good approximation for wells which are not square, we would have a rather shape-independent method for

estimating the radial integrals from a knowledge of the level scheme.

To see whether such a method is feasible, consider a potential which is $-V_0$ for $r \leq (R_0 - a)$ and then rises with constant slope to zero at $r = (R_0 + a)$. By using perturbation theory, one can show^{29,49} that the radial integral (B4) is approximately

$$(-1)^{n-n'}[\langle T \rangle_{nl}\langle T \rangle_{n'l'}]^{1/2}(1 + D\delta^2 + \dots), \quad (\text{B9})$$

where $\delta = (a/R_0)$. From an estimate of D and the fact that K_{nl} is a slowly varying function of the binding energy, we conclude that if $\delta \lesssim 0.1$, one may determine the radial integrals of $rV'(r)$ from (B4). The value of K_{nl} which is used in (B4) is taken from Fig. 7 in conjunction with our *ad hoc* level scheme of Fig. 3, it being assumed that the level $3d_{3/2}$ is just bound.

In order to simplify the construction of the matrix of Eq. (17), we dropped the term of \mathcal{W}_2 proportional to $[Y_{20}(\theta)]^2$, and corrected the eigenvalues obtained from the diagonalization by computing the expectation value of this term with the states χ_α . These corrections turn out to be very small, and so this procedure would appear to be justified. The levels shown in Fig. 4 already include this correction.⁵⁰

APPENDIX III

We have

$$\langle j_{z'} \rangle_{M=I} = I^2(I+1)^{-1} \quad (\Omega = K = I \neq \frac{1}{2}), \quad (\text{C1})$$

$$= \frac{1}{2}(I+1)^{-1}[\frac{1}{2} - (-1)^{I+\frac{1}{2}}(I+\frac{1}{2})a_k] \quad (\Omega = K = \frac{1}{2}). \quad (\text{C2})$$

In the following we shall suppress the indices k, n in $C_\Omega^w(k\beta|nj)$, as well as the variable β , and replace j by $(l \pm \frac{1}{2})$. Then for $\Omega = K \neq \frac{1}{2}$,

$$\begin{aligned} \langle s_{z'} \rangle_{M=I} = & \frac{\Omega}{I+1} \sum_{nl} (2l+1)^{-1} \\ & \times \{ \Omega |C_\Omega^w(l+\frac{1}{2})|^2 - \Omega |C_\Omega^w(l-\frac{1}{2})|^2 \\ & - 2[(l+\Omega+\frac{1}{2})(l-\Omega+\frac{1}{2})]^{1/2} \\ & \times C_\Omega^w(l+\frac{1}{2})C_\Omega^w(l-\frac{1}{2}) \}; \quad (\text{C3}) \end{aligned}$$

⁴⁹ An error in reference 29, relevant to Eq. (B9), has kindly been brought to our attention by K. Kumar.

⁵⁰ Note added in proof.—Several criticisms of the approximation embodied in Eq. (14) have kindly been brought to the author's attention by Mr. K. Kumar. The most important of these is that for $\theta < 30^\circ$ the quadratic approximation has strong fluctuations, which the exact potential does not possess. The author has therefore computed several matrix elements of the type which appear in Eq. (17), by using the exact expression [Eq. (B1)], and also the approximate one [Eq. (14)], the potential being the one used to describe elastic proton scattering. He finds that if one interprets Eq. (14) as the description of a prolate deformation which differs but slightly from a spheroid, the expansion gives results which agree tolerably well with those obtained from a correspondingly changed but closed expression. These changes in the details of the shape of the equipotential surfaces are completely compatible with present experimental evidence. The author therefore concludes that the final results (see Table III) are not effected by the shortcomings of Eq. (14). It is, however, quite probable that this approximation is quite poor for $\beta < -0.2$. Professor J. D. Jackson's help in this matter is gratefully acknowledged.

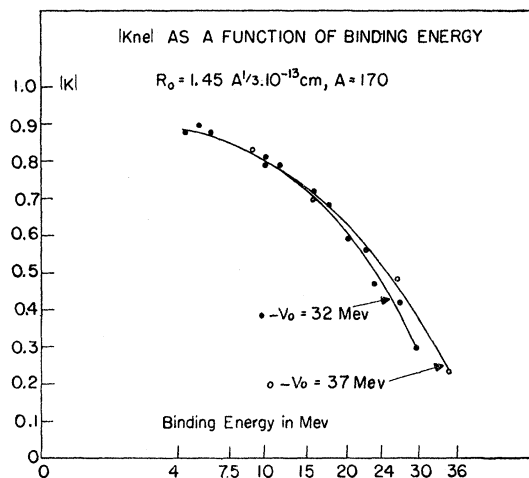


FIG. 7. K_{nl} , the radial integral defined in Appendix II, as a function of binding energy.

while for $\Omega = K = \frac{1}{2}$,

$$\begin{aligned} \langle s_z \rangle_{M=I} = (I+1)^{-1} \{ & \frac{1}{4} \sum_{nl} n_l (2l+1)^{-1} \{ |C_{\frac{1}{2}}^w(l+\frac{1}{2})|^2 \\ & - |C_{\frac{1}{2}}^w(l-\frac{1}{2})|^2 - 4[l(l+1)]^{\frac{1}{2}} C_{\frac{1}{2}}^w(l+\frac{1}{2}) \\ & \times C_{\frac{1}{2}}^w(l-\frac{1}{2}) \} - \frac{1}{2} w (-1)^{I+\frac{1}{2}} (I+\frac{1}{2}) \\ & \times \sum_{nl} n_l (2l+1)^{-1} [l^{\frac{1}{2}} C_{\frac{1}{2}}^w(l-\frac{1}{2}) \\ & - (l+1)^{\frac{1}{2}} C_{\frac{1}{2}}^w(l+\frac{1}{2})]^2 \}. \quad (C4) \end{aligned}$$

When $I = \frac{1}{2}$, (C4) reduces to

$$\begin{aligned} \frac{1}{6} \sum_{nl} n_l (2l+1)^{-1} \{ & (2l+3) |C_{\frac{1}{2}}^w(l+\frac{1}{2})|^2 \\ & + (2l-1) |C_{\frac{1}{2}}^w(l-\frac{1}{2})|^2 \\ & - 8[l(l+1)]^{\frac{1}{2}} C_{\frac{1}{2}}^w(l+\frac{1}{2}) C_{\frac{1}{2}}^w(l-\frac{1}{2}) \} \quad (C5) \end{aligned}$$

for $w=1$, and is simply equal to $-\frac{1}{6}$ when $w=-1$. In the latter case, we simply get Nilsson's result³⁰

$$\mu = \frac{1}{3} [(g_l - g_c) a_k + g_l + g_c - \frac{1}{2} g_s]. \quad (C6)$$

This formula makes it possible to determine the parity of some rotational bands which have $I_0 = \frac{1}{2}$. For if one knows both μ and a_k , and finds that they are not related through (C6), one can conclude that $w = +1$. It is in this way that we have assigned even parity to the ground states of W^{183} and Tm^{169} ; see Table III, footnote e.

PHYSICAL REVIEW

VOLUME 103, NUMBER 4

AUGUST 15, 1956

Inelastic Scattering of Neutrons*

IRA L. MORGAN

Department of Physics, University of Texas, Austin, Texas

(Received May 14, 1956)

Inelastic scattering of fast neutrons in Al, Na, S, Fe, Cu, I, and Cd has been detected by observing the gamma radiation from the excited states. The cross sections for gamma-ray production at energies well above threshold in Fe and Al have been measured. The gamma-ray energies observed correspond to known levels, transitions between levels, or de-excitation from neutron capture.

INTRODUCTION

A WELL-KNOWN method for investigating the levels in light, medium, and heavy nuclei is by the inelastic scattering of neutrons. This process involves the interaction of a neutron with the nucleus in which the de-excitation of the nucleus is by gamma-ray emission accompanied by an inelastically scattered neutron. If the level of excitation is high enough, cascade between levels may occur. Competing processes also have a direct influence on the excitation curve. Many investigators¹⁻⁴ have studied the resulting gamma radiation due to inelastically scattered neutrons. In general this has been at one energy or in the region of threshold for production of the gamma radiation. In the present investigation, the shape of the excitation curves at energies well above threshold has been obtained in order to study the effect of additional cascading from higher levels, as well as competing reactions. The energy of the gamma radiation observed in this work is consistent with known energy levels, capture processes, or cascades between levels.

EXPERIMENTAL PROCEDURE

The University of Texas Van de Graaff generator was used to produce the reactions $D(d,n)He^3$ and $Li^7(p,n)Be^7$, providing neutrons in the energy range

* Assisted by the U. S. Atomic Energy Commission.

¹ M. A. Rothman and C. E. Mandeville, Phys. Rev. **93**, 796 (1954).

² R. M. Kiehn and C. Goodman, Phys. Rev. **92**, 652 (1953).

³ Scherrer, Allison, and Faust, Phys. Rev. **96**, 386 (1954).

⁴ J. J. Van Loef and D. A. Lind, Phys. Rev. **101**, 103 (1956).

required. A deuterium gas cell was used which was 2 cm in depth with a 0.0001-in. Ni foil covering the entrance hole which passed the deuteron beam. The Li^7 target was evaporated on a silver backing and was found to be 35 kev thick as measured by the threshold method.

A "ring" geometry was used and found to be convenient for those elements studied, producing high intensities and a low background. Metallic Na was shaped in the form of a ring and contained in kerosene, except during periods of bombardment. Sulfur was melted and molded into a ring, while iodine in the form of crystals was packed in a thin-wall hollow Al ring. The other elements were easily machined. The attenuators, which were conical in shape, were of paraffin or

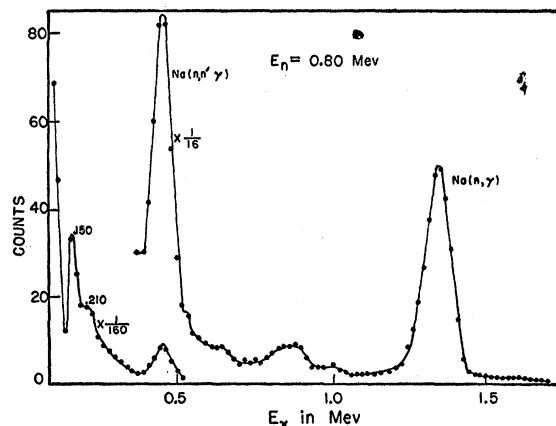


FIG. 1. Pulse-height distribution of the gamma rays produced by 800-kev neutron bombardment of Na.